2016

β -NMR Investigation of the Depth-Dependent Magnetic Properties of an Antiferromagnetic Surface

David L. Cortie
University of British Columbia, dlc422@uowmail.edu.au

T Buck
University of British Columbia

M Dehn
Technische Universitat Munchen

V L. Karner
University of British Columbia

R F. Kiefl
Triumf, University of British Columbia

See next page for additional authors

Publication Details

Cortie, D. L., Buck, T., Dehn, M. H., Karner, V. L., Kiefl, R. F., Levy, C. D. P., Mcfadden, R. M.L., Morris, G. D., McKenzie, I., Pearson, M. R., Wang, X. L. & Macfarlane, W. A. (2016). β -NMR Investigation of the Depth-Dependent Magnetic Properties of an Antiferromagnetic Surface. Physical Review Letters, 116 106103-1-106103-5.

β -NMR Investigation of the Depth-Dependent Magnetic Properties of an Antiferromagnetic Surface

Abstract
By measuring the prototypical antiferromagnet α-Fe2O3, we show that it is possible to determine the static spin orientation and dynamic spin correlations within nanometers from an antiferromagnetic surface using the nuclear spin polarization of implanted 8Liþ ions detected with β-NMR. Remarkably, the firstorder Morin spin reorientation in single crystal α-Fe2O3 occurs at the same temperature at all depths between 1 and 100 nm from the (110) surface; however, the implanted nuclear spin experiences an increased 1=T1 relaxation rate at shallow depths revealing soft-surface magnons. The surface-localized dynamics decay towards the bulk with a characteristic length of ϵ ¼ 11 1 nm, closely matching the finite-size thresholds of hematite nanostructures.

Keywords
nmr, antiferromagnetic, magnetic, surface, properties, investigation, depth, dependent

Disciplines
Engineering | Physical Sciences and Mathematics

Publication Details
Cortie, D. L., Buck, T., Dehn, M. H., Karner, V. L., Kiefl, R. F., Levy, C. D. P., Mcfadden, R. M.L., Morris, G. D., McKenzie, I., Pearson, M. R., Wang, X. L. & Macfarlane, W. A. (2016). β -NMR Investigation of the Depth-Dependent Magnetic Properties of an Antiferromagnetic Surface. Physical Review Letters, 116 106103-1-106103-5.

Authors
David L. Cortie, T Buck, M Dehn, V L. Karner, R F. Kiefl, C D. P Levy, R M. L Mcfadden, G D. Morris, I McKenzie, M R. Pearson, Xiaolin Wang, and W A. Macfarlane

β-NMR Investigation of the Depth-Dependent Magnetic Properties of an Antiferromagnetic Surface

D. L. Cortie,[1,2,3,4] T. Buck,[5] M. H. Dehn,[6] V. L. Karner,[5] R. F. Kiefl,[2,1,4] C. D. P. Levy,[4] R. M. L. McFadden,[3] G. D. Morris,[4] I. McKenzie,[4] M. R. Pearson,[4] X. L. Wang,[7] and W. A. MacFarlane[3,1]

[1]*Quantum Matter Institute, University of British Columbia, Vancouver, British Columbia V6T 1Z1, Canada*
[2]*Department of Physics and Astronomy, University of British Columbia, Vancouver, British Columbia V6T 1Z1, Canada*
[3]*Chemistry Department, University of British Columbia, Vancouver, British Columbia V6T 1Z1, Canada*
[4]*TRIUMF, 4004 Wesbrook Mall, Vancouver, British Columbia V6T 2A3, Canada*
[5]*Department of Physics and Astronomy, University of British Columbia, Vancouver, British Columbia V6T 1Z1, Canada*
[6]*Physik-Department, Technische Universität München, 85748 Garching bei München, Germany*
[7]*Institute for Superconducting and Electronic Materials, University of Wollongong, NSW 2500, Australia*

(Received 15 August 2015; revised manuscript received 27 January 2016; published 10 March 2016)

By measuring the prototypical antiferromagnet α-Fe_2O_3, we show that it is possible to determine the static spin orientation and dynamic spin correlations within nanometers from an antiferromagnetic surface using the nuclear spin polarization of implanted $^8Li^+$ ions detected with β-NMR. Remarkably, the first-order Morin spin reorientation in single crystal α-Fe_2O_3 occurs at the same temperature at all depths between 1 and 100 nm from the (110) surface; however, the implanted nuclear spin experiences an increased $1/T_1$ relaxation rate at shallow depths revealing soft-surface magnons. The surface-localized dynamics decay towards the bulk with a characteristic length of $\epsilon = 11 \pm 1$ nm, closely matching the finite-size thresholds of hematite nanostructures.

DOI: 10.1103/PhysRevLett.116.106103

In the textbook case of an infinite "bulk" magnet, any phase transition can be categorized as first order or second order, and there is a causal relationship between the spin dynamics and the transition temperature. Near a surface, however, the character of a phase transition is modified by broken translational symmetry. If the bulk transition is second order, then the near-surface region typically exhibits altered critical exponents allowing for the classification of surface critical phenomena into four universal types: ordinary, surface, special, and extraordinary [1,2]. In contrast, even if the bulk transition manifests as a first-order jump, the surface region may "dewet" to form a distinct layer exhibiting gradual second-order behavior over a characteristic depth describing surface-induced order or disorder [1,3]. This general hierarchy has been widely used to classify near-surface phase transitions; however, there is mounting experimental evidence that antiferromagnetic materials present additional complexity at nanometer-scale interfaces [4–6]. Here, we report that the near-surface behavior of the spin reorientation (SR) transition in a prototypical antiferromagnet (AFM) α-Fe_2O_3 evades classification according to the above heirachy, reflecting a new phenomenon which we term a latent surface transition. The defining feature of such a transition is that the free-energy relation is modified near the surface without causing a distinct dewetting from the bulk order parameter in the semi-infinite system. Instead, the driving dynamics are altered over a characteristic length scale setting the threshold for surface transitions in finite-size systems. In bulk antiferromagnets, low energy magnons mediate SR [7,8], and we present compelling evidence for the existence of localized soft magnons near a surface. This is a key step towards explaining certain anomalous spin reorientations in finite-size antiferromagnets.

To study the near-surface antiferromagnetic properties, we used a nuclear-detected magnetic resonance method (β-NMR). This is the first application of this depth-resolved ion-beam technique to detect the NMR signal from the near-surface region of an antiferromagnet. The noncubic antiferromagnet α-Fe_2O_3 ($R\bar{3}c$) represents the ideal test case because it displays an abrupt SR at the Morin temperature ($T_M = 260 \pm 5$ K), far below the Néel transition ($T_N = 949 \pm 10$ K), which is known to be associated with the softening of a key magnon mode [9,10] and is theorized to show nontrivial magnetic surface states [7]. The staggered magnetization $\vec{M}$ points along the hexagonal (001) direction for $T < T_M$, whereas $\vec{M}$ is perpendicular to the latter direction for $T > T_M$. In the experiment, a beam of radioactive $^8Li^+$ from the ISAC facility at TRIUMF [11] was first spin polarized in-flight using collinear optical pumping [12]. The beam was then implanted into a (110)-oriented α-Fe_2O_3 crystal at kinetic energies ranging from 1–20 keV. The highly polished crystal from SurfaceNet GmbH (Rheine, Germany) had a low surface roughness (0.6 ± 0.2 nm) and a low mosaic spread (0.06 deg). The probing depth of the $^8Li^+$ ensemble is related to the implantation energy and was modeled using the Stopping Range of Ions in Matter software (SRIM) [13]. The nuclear

spin polarization vector $\vec{P}$ is fixed perpendicular to the beam path, such that its relative direction in the crystal can be changed by reorienting the sample. The asymmetric emission of the radioactive β decay products is proportional to $\vec{P}$ at the time of the decay of the $^8Li^+$ (spin $I = 2$), which has a mean lifetime $\tau = 1.21$ s. Similar to the better-known μSR, the radioactive spin probe stops in the crystal, where it senses its surroundings via hyperfine interactions [14]. In a magnetically ordered state, this results in a static (time-averaged) hyperfine field at the $^8Li^+$ nucleus: the local field $\vec{H}_L$ [15]. Any component of $\vec{P}$ perpendicular to $\vec{H}_L$ precesses rapidly and averages to zero. Whereas the parallel component does not precess, it will gradually decay by spin-lattice relaxation to an equilibrium close to zero. The rate of this relaxation, $1/T_1$, is mainly determined by the fluctuating part of $\vec{H}_L$ perpendicular to $\vec{P}$, with frequencies close to the nuclear Larmor frequency [16,17].

The spin-reorientation transition causes a sharp change in the nuclear polarization shown by the spin-lattice-relaxation signal [see Fig. 1(a)]. In the latter measurement, four-second beam pulses of ions at 20 keV were implanted at a mean depth of 85 nm. No external static or rf field is applied in the measurement, allowing the $^8Li^+$ spin to relax naturally under perturbations from the surrounding environment. The 261 K data show that the polarization of the ensemble of $^8Li^+$ is completely destroyed when $\vec{P}\|(001)$, consistent with a local field $\vec{H}_L\perp(001)$. A large polarization (asymmetry) of the $^8Li^+$ is suddenly recovered when the sample is cooled through the transition to 259 K, as $\vec{H}_L$ is now along $\vec{P}$. The change is consistent with $\vec{H}_L\|\vec{M}$, the sublattice magnetization. Thus, the antiferromagnetic orientation acts as an effective spin filter for the $^8Li^+$, either preserving or destroying the initial polarization, making it very sensitive to the direction of $\vec{M}$. The surviving polarization $A(t)$ of the $^8Li^+$ ensemble decreases slowly over several seconds due to fluctuations of $\vec{H}_L$ which drive spin-lattice relaxation. This process is described using a stretched exponential relaxation convoluted with the beam pulse of length $t_0 = 4$ s [18]:

$$A(t) = \begin{cases} \frac{1}{N}\int_0^t e^{-(t-t')/\tau} p(t,t')dt', & t \le t_0 \\ \frac{1}{N}\int_0^t e^{-(t_0-t')/\tau} p(t,t')dt', & t > t_0, \end{cases} \quad (1)$$

with $p(t,t':1/T_1^*,A_0) = A_0 e^{-[(t-t')/T_1^*]^\beta}$, and the normalizing factor $N(t) = \int_0^t e^{-t'/\tau}dt'$. The data are well described with a stretching exponent $\beta = 0.35 \pm 0.05$, with the caveat that both $1/T_1^*$ and A_0 are T dependent. The stretched exponential describes a distribution of relaxation times caused by the interaction with magnetic fluctuations, where the inverse average relaxation time is $1/T_1 = (\beta/T_1^*)\{1/[\Gamma(1/\beta)]\}$ and Γ is the gamma function [19]. Although the spin-lattice-relaxation rate $(1/T_1)$ is on the scale of seconds, the antiferromagnetic dynamics causing the relevant nuclear transitions occur at $\approx 10^{-7}$ s time scales to produce spontaneous fields matching the nuclear Larmor frequency (9.5 MHz at 1.5 T) [16,17]. The variable value of the initial asymmetry A_0 encapsulates the nonprecessing nuclear spin component $A_0 \propto \cos^2\theta$, where $\cos\theta \propto \vec{P}\cdot\vec{H}_L$, and thus is sensitive only to the static internal field. The steplike drop in A_0 above 260 K is caused by the first-order Morin transition where $\theta' = \theta + 90°$. To confirm this, Fig. 1(b) shows that rotating the crystal such that $P\|(1\bar{1}0)$ alters the component of $\vec{M}$ on $\vec{P}$ above T_M, giving a finite asymmetry in the resulting configuration, as expected. The tenfold reduction is a signature of degenerate domains forming in the basal plane together with weak ferromagnetism. Figure 1(c) summarizes the initial asymmetry A_0 as a function of temperature for the two orientations. The spin-reorientation temperature is manifest as a sudden jump in the value of observable asymmetry (A_0), providing a model-independent method to monitor changes in the antiferromagnetic orientation.

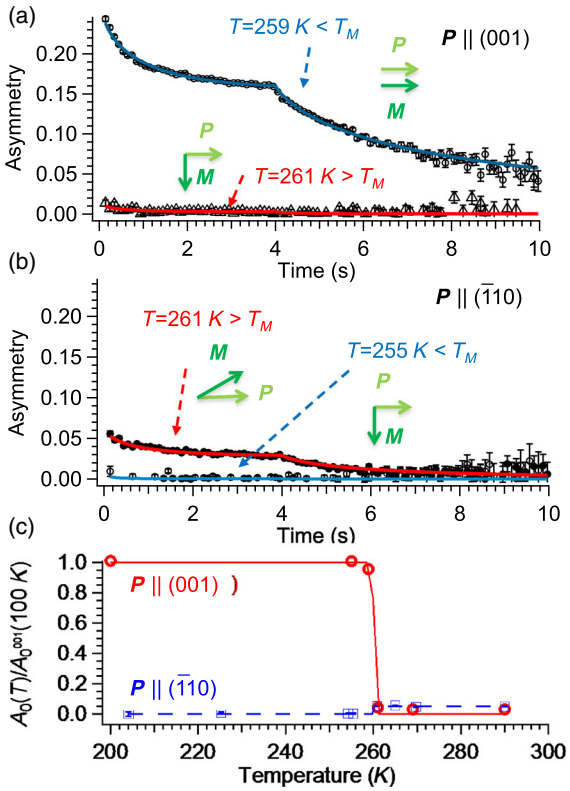

FIG. 1. Spin-lattice-relaxation measurements of $^8Li^+$ implanted at 20 keV into an α-Fe_2O_3 crystal show a step in the observable nuclear polarization at the SR transition ($T_M = 260$ K) for two rotations of the crystal such that (a) $\vec{P}\|(001)$ and (b) $\vec{P}\|(\bar{1}10)$. The curves have not been offset or scaled. The kink at 4 s in (a) and (b) is the end of the incoming $^8Li^+$ pulse. The antiferromagnetic spin reorientation is evident in (c) as a step in the initial asymmetry A_0 as a function of temperature.

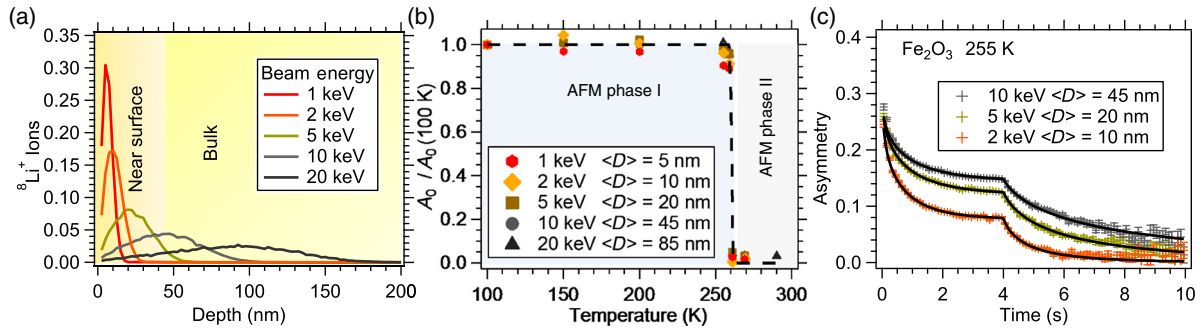

FIG. 2. (a) Stopping profile of $^8Li^+$ ions as a function of beam energy calculated with SRIM. (b) Initial experimental asymmetry A_0 as a function of temperature for several beam energies. The steplike decrease signifies the SR transition. (c) Sample β-NMR SLR data as a function of beam energy below the Morin transition showing modified spin-lattice relaxation for ions stopping near the α-Fe_2O_3 (110) surface.

The depth-resolved β-NMR shows that the near-surface antiferromagnetic structure reorients at the same temperature as the bulk Morin transition; however, the spin dynamics are strongly surface modified. To observe this, it is necessary to selectively probe regions within a few nanometers of the surface through the choice of $^8Li^+$ implantation energy, as shown in the simulated profiles in Fig. 2(a). Contrary to theoretical predictions, the antiferromagnetic orientation is depth independent between 1 and 200 nm at temperatures near T_M. As shown in Fig. 2(b), the experimental asymmetry A_0 of $^8Li^+$ at different depths exhibits the same behavior, where the step at 260 K is the bulk T_M, and the transition retains a first-order character near the surface. For instance, in Fig. 2(c), as $t \to 0$, there are no significant differences in the value of A_0 that would signify a fraction of $^8Li^+$ in a surface spin-flop domain. Any change in the direction of the internal field would alter the magnitude of the nonprecessing component, indicating that the $^8Li^+$'s experience the same internal field direction at all depths, ruling out a noncollinear spiral structure.

The identical transition temperature differs from several theories proposing that spin reorientation of a free antiferromagnetic surface is intrinsically different from the bulk [7,20], even acting as the initial trigger for the bulk [21]. The dominant first-order behavior is similar, within experimental uncertainty, to past findings from Mössbauer spectroscopy [22,23], and it is different than models of the hematite surface which propose a strongly second-order transition [20] or a nucleating spin-flop domain [7]. This surface insensitivity is surprising because it is widely known that the spin-reorientation temperature is suppressed in nanoparticles [24–26] and thin films [27,28]. A universal explanation would be a suppressed surface transition temperature [7], but there is no evidence of this in the semi-infinite case. Two other explanations have been offered: finite-size [29] and lattice distortion [30]. While we discount lattice strain in our crystal, we find evidence of a finite length scale implicit in the antiferromagnetic dynamics illustrated in Fig. 2(c), which shows spin-relaxation measurements at 255 K for several depths. Clearly, the nuclear spins relax very differently depending on proximity to the surface. In α-Fe_2O_3, the depth-dependent $1/T_1$ signifies modified antiferromagnet dynamics [16] with a higher spectral density near the surface. One theory predicted the existence of magnetic surface states on α-Fe_2O_3 accompanied by soft-surface magnons [7], motivated by earlier calculations showing that dipolar anisotropy makes a large contribution to the net anisotropy field [31]. The existence of a modified excitation spectrum in finite-size α-Fe_2O_3 has recently been observed by inelastic neutron spectroscopy (INS) in powders of nanoparticles [24–26]. The latter linked the surface spin dynamics to a modified surface anisotropy [26], which alters the free-energy relation, acting to decrease the Morin transition to below 2.2 K in hematite nanoparticles [24–26]. The precise depth and homogeneity of the relevant spin excitations, however, has not been determined until now due to the volume-averaged nature of INS. The decay depth is important, however, because it reveals the spatial scale where variations in the local free-energy relationship occur, and thus it sets a threshold where surface-dominated behavior is expected in nanomaterials. In order to determine the length scale of the surface-localized antiferromagnetic dynamics, the temperature dependence of the magnetic excitation was recorded for several beam energies. Figure 3(a) shows the depth dependence of the average $1/T_1$ measured approaching T_M from a lower temperature. The relaxation rate decreases exponentially from the surface with a temperature-independent length scale $\epsilon = 11 \pm 1$ nm that does not diverge near T_M. The absence of a diverging correlation length again confirms that the latter is not a typical second-order surface transition. As discussed, the modified dynamics do not alter the surface phase transition temperature in the semi-infinite crystal, indicating that coupling of the top layers of spins to the underlying bulk layers acts to globally enforce the ordinary transition temperature. Nevertheless, the specific length scale where we observe modified dynamics is illuminating in the context of the rich data set [32–37] which shows a suppressed Morin temperature in finite-size

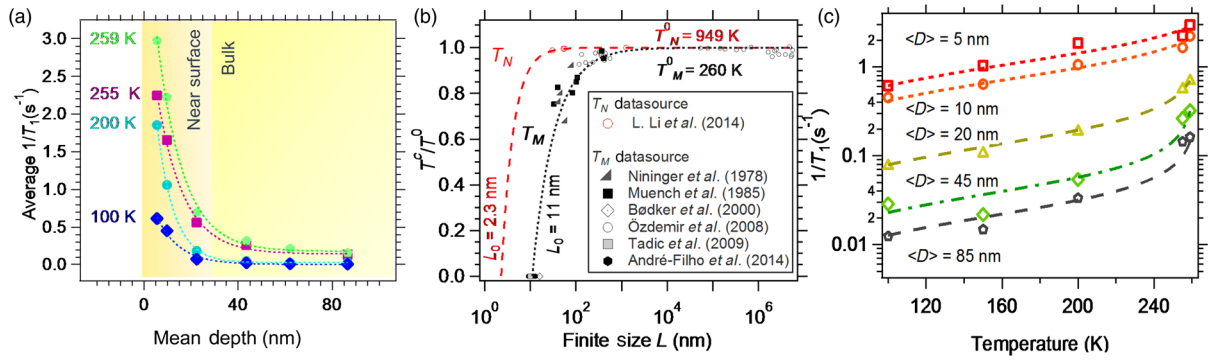

FIG. 3. (a) The nuclear relaxation rate $1/T_1$ is depth dependent near the (110) α-Fe_2O_3 surface, with a characteristic decay length of 11 nm. (b) Data-mined experimental results for spherical α-Fe_2O_3 nanoparticles taken from the previously published references showing the finite-size threshold for the Néel and Morin phase transition are approximately 2.3 and 11 nm, respectively. (c) Temperature dependence of the β-NMR $1/T_1$ rate at the surface of the α-Fe_2O_3 crystal at different depths, implying that the relaxation is caused by soft-surface magnons, described by the model encapsulated in Eqs. (3) and (2).

hematite particles [see Fig. 3(b)]. From this data mining, it is clear that the Morin temperature is strongly dependent on the finite particle length L and is typically suppressed below 5 K for $L < 10$ nm [30,34]. In contrast to the latter strong effect on T_M, finite size only weakly affects the second-order Néel transition. Recent high-T data on hematite nanostructures indicates that T_N obeys the standard form $(T_c/T_0) = 1 - (L_0/L)^{1/\nu}$ governed by a typical suppression length $L_0 = 2.3$ nm, and a scaling exponent near the Ising value $\nu = 0.6$ [38]. Applying the same form to the Morin transition, Fig. 3(b) shows that the first-order T_M scaling is governed by a much larger length scale $L_0 = 11$ nm and a higher scaling exponent ($\nu \approx 1.0$). It is remarkable that the spatial scale governing the SR transition in the zero-dimensional particles matches that of the modified dynamics at the semi-infinite three-dimensional surface. This implies a phase transition controlled by a modified surface-free-energy relation rather than short-range surface critical behavior. Clearly, the suppressed transition remains "latent" in the semi-infinite limit, but it is present in dimensionally constrained α-Fe_2O_3 nanoparticles [32–37] or 2D films [6,39] with a length scale below ϵ.

The origin of the modified dynamics provides insight into which parameters change in the surface free energy. Our temperature-dependent $1/T_1$ measurements indicate that modified spin dynamics arise from altered surface magnon behavior near the transition, caused by the change in surface anisotropy which controls the energy of soft modes related to the reorientation [9,10]. Theories have been developed for the relaxation of a nuclear spin due to hyperfine interactions with a thermal population of antiferromagnetic magnons [16,40]. Energy conservation constrains the interaction between the nuclear and electron spins. The direct process, whereby a single magnon is scattered from the nuclear spin, is typically forbidden because a small spin anisotropy will gap (Δ) the magnon spectrum with a forbidden region extending far above the nuclear Larmor frequency (sub-μeV range). The lowest energy magnon mode in hematite occurs at the finite gap energy [10]:

$$\Delta(T, D) = \hbar\omega_{LO}(0)\left[1 - \left(\frac{T}{T_L}\right)^4\right]^{1/2}, \tag{2}$$

with $\omega_{LO}(0) \approx 1$ THz, and $\Delta(T, D) \approx 0.1$ THz at 260 K for bulk ($D = \infty$), where D is the depth from the surface. The incomplete softening has been explained as resulting in $T_L = T_M(1 + \delta)$, where δ is a coefficient related to the net magnetic anisotropy [9]. Without zero-energy excitations, nuclear relaxation in an antiferromagnet occurs by a multimagnon process, corresponding to the absorption and emission of magnons with different energies. This mechanism is sensitive to spin waves over the entire Brillouin zone; however, INS [41] and Raman spectroscopy [42] show that the bulk high energy magnons barely change above and below T_M in α-Fe_2O_3. Therefore, to a first approximation, we relate the changes in T_1 to the occupation of soft modes above the anisotropy gap, obtaining the simplified relation

$$T_1(D) = \frac{[e^{\Delta(T,D)/k_BT} - 1]}{AM_0(D)}. \tag{3}$$

M_0 accounts for a rigid magnon density of states thermally populated across a depth-dependent Δ obeying Eq. (2), and A is a proportionality constant accounting for the hyperfine coupling. Figure 3(c) illustrates that the model based on Eq. (3) produces a reasonable description of the bulk and surface nuclear relaxation in the temperature range 100–260 K, using the common Morin transition $T_M = 260$ K. A key result from the model is that the fitted δ value—even at 85 nm deep—is 0.016 ± 0.02, which is slightly smaller than the bulk anisotropy parameter reported in the range 0.02–0.04 [10]. Interestingly, δ is significantly increased near the surface to 0.08 ± 0.03 at 10 nm, supporting the theory of strong changes in the hematite

surface anisotropy on nanometer length scales [7]. Néel proposed that magnetic surface anisotropy is a universal feature of antiferromagnets, although the strength and range of this interaction remains largely untested [43].

In conclusion, these results show convincingly that β-NMR can measure phase transitions, structure, and dynamics near antiferromagnetic interfaces, thereby providing a new tool for optimizing spin-based functionality. The observation of modified dynamics, linked to surface anisotropy, suggests a method for designing antiferromagnetic correlations in thin film heterostructures.

This research was performed at the Centre for Materials and Molecular Science, supported by TRIUMF, the National Research Council and the NSERC of Canada. X. L. acknowledges the Australian Research Council. The authors thank M. Gingras for valuable discussions.

[1] H. Dosch, in *Critical Phenomena at Surfaces and Interfaces: Evanescent X-Ray and Neutron Scattering*, Springer Tracts in Modern Physics Vol. 126, edited by G. Hohler (Springer-Verlag, Berlin, 1992).
[2] M. Pleimling, J. Phys. A **37**, R79 (2004).
[3] R. Lipowsky, Phys. Rev. Lett. **49**, 1575 (1982).
[4] S. J. Lee, J. P. Goff, G. J. McIntyre, R. C. C. Ward, S. Langridge, T. Charlton, R. Dalgliesh, and D. Mannix, Phys. Rev. Lett. **99**, 037204 (2007).
[5] R. Morales, Z.-P. Li, J. Olamit, K. Liu, J. M. Alameda, and I. K. Schuller, Phys. Rev. Lett. **102**, 097201 (2009).
[6] S. Park, H. Jang, J.-Y. Kim, B.-G. Park, T.-Y. Koo, and J.-H. Park, Europhys. Lett. **103**, 27007 (2013).
[7] H. Chow and F. Keffer, Phys. Rev. B **10**, 243 (1974).
[8] E. Constable, D. L. Cortie, J. Horvat, R. A. Lewis, Z. Cheng, G. Deng, S. Cao, S. Yuan, and G. Ma, Phys. Rev. B **90**, 054413 (2014).
[9] O. Nagai, N. L. Bonavito, and T. Tanaka, J. Phys. C **8**, 176 (1975).
[10] S. G. Chou, P. E. Stutzman, S. Wang, E. J. Garboczi, W. F. Egelhoff, and D. F. Plusquellic, J. Phys. Chem. C **116**, 16161 (2012).
[11] P. Bricault, F. Ames, T. Achtzehn, M. Dombsky, F. Labrecque, J. Lassen, J.-P. Lavoie, and N. Lecesne, Rev. Sci. Instrum. **79**, 02A908 (2008).
[12] C. D. P. Levy, M. Pearson, R. F. Kiefl, E. Mané, G. D. Morris, and A. Voss, Hyperfine Interact. **225**, 165 (2014).
[13] J. F. Ziegler and J. P. Biersack, in *Treatise on Heavy-Ion Science*, edited by D. A. Bromley (Springer, New York, 1985), p. 93.
[14] W. MacFarlane, Solid State Nucl. Magn. Reson. **68–69**, 1 (2015).
[15] Our measurements as a function of the applied field indicate that $|\vec{H}_L|$ is on the order of 1.5 T in hematite.
[16] T. Moriya, Prog. Theor. Exp. Phys. **16**, 23 (1956).
[17] D. L. Cortie, T. Buck, M. H. Dehn, R. F. Kiefl, C. D. P. Levy, R. M. L. McFadden, G. D. Morris, M. R. Pearson, Z. Salman, Y. Maeno, and W. A. MacFarlane, Phys. Rev. B **91**, 241113 (2015).
[18] Z. Salman, O. Ofer, M. Radovic, H. Hao, M. Ben Shalom, K. H. Chow, Y. Dagan, M. D. Hossain, C. D. P. Levy, W. A. MacFarlane, G. M. Morris, L. Patthey, M. R. Pearson, H. Saadaoui, T. Schmitt, D. Wang, and R. F. Kiefl, Phys. Rev. Lett. **109**, 257207 (2012).
[19] I. McKenzie, M. Harada, R. F. Kiefl, C. D. P. Levy, W. A. MacFarlane, G. D. Morris, S.-I. Ogata, M. R. Pearson, and J. Sugiyama, J. Am. Chem. Soc. **136**, 7833 (2014).
[20] M. I. Kaganov, J. Exp. Theor. Phys. **52**, 779 (1980).
[21] F. Keffer and H. Chow, Phys. Rev. Lett. **31**, 1061 (1973).
[22] T. Shinjo, M. Kiyama, N. Sugita, K. Watanabe, and T. Takada, J. Magn. Magn. Mater. **35**, 133 (1983).
[23] A. Kamzin and D. Vcherashnii, J. Exp. Theor. Phys. **75**, 575 (2002).
[24] L. Theil Kuhn, K. Lefmann, C. R. H. Bahl, S. Nyborg Ancona, P.-A. Lindgård, C. Frandsen, D. E. Madsen, and S. Mørup, Phys. Rev. B **74**, 184406 (2006).
[25] S. N. Klausen, K. Lefmann, P.-A. Lindgård, L. Theil Kuhn, C. R. H. Bahl, C. Frandsen, S. Mørup, B. Roessli, N. Cavadini, and C. Niedermayer, Phys. Rev. B **70**, 214411 (2004).
[26] A. H. Hill, H. Jacobsen, J. R. Stewart, F. Jiao, N. P. Jensen, S. L. Holm, H. Mutka, T. Seydel, A. Harrison, and K. Lefmann, J. Chem. Phys. **140**, 044709 (2014).
[27] J. Dho, C. W. Leung, Z. H. Barber, and M. G. Blamire, Phys. Rev. B **71**, 180402 (2005).
[28] D. L. Cortie, K.-W. Lin, C. Shueh, H.-F. Hsu, X. L. Wang, M. James, H. Fritzsche, S. Brück, and F. Klose, Phys. Rev. B **86**, 054408 (2012).
[29] X. Y. Lang, W. T. Zheng, and Q. Jiang, Phys. Rev. B **73**, 224444 (2006).
[30] D. Schroeer and R. C. Nininger, Phys. Rev. Lett. **19**, 632 (1967).
[31] J. O. Artman, J. C. Murphy, and S. Foner, Phys. Rev. **138**, A912 (1965).
[32] R. C. Nininger and D. Schroeer, J. Phys. Chem. Solids **39**, 137 (1978).
[33] F. Bødker, M. F. Hansen, C. B. Koch, K. Lefmann, and S. Mørup, Phys. Rev. B **61**, 6826 (2000).
[34] O. Özdemir, D. J. Dunlop, and T. S. Berquò, Geochem., Geophys., Geosyst. **9**, Q10Z01 (2008).
[35] J. Andr-Filho, L. Len-Flix, J. Coaquira, V. Garg, and A. Oliveira, in *LACAME 2012*, edited by C. Meneses, E. Caetano, C. Torres, C. Pizarro, and L. Alfonso (Springer, Dordrecht, 2014), p. 183.
[36] G. J. Muench, S. Arajs, and E. Matijevi, Phys. Status Solidi A **92**, 187 (1985).
[37] M. Tadic, V. Kusigerski, D. Markovic, I. Milosevic, and V. Spasojevic, J. Magn. Magn. Mater. **321**, 12 (2009).
[38] L. Li, F.-g. Li, J. Wang, and G.-m. Zhao, J. Appl. Phys. **116**, 174301 (2014).
[39] S. Gota, M. Gautier-Soyer, and M. Sacchi, Phys. Rev. B **64**, 224407 (2001).
[40] D. Beeman and P. Pincus, Phys. Rev. **166**, 359 (1968).
[41] E. J. Samuelsen and G. Shirane, J. Phys. (Paris), Colloq. **32**, C1-1064 (1971).
[42] Y. Tanabe, Y. Fujimaki, K. Kojima, S. Uchida, S. Onari, T. Matsuo, S. Azuma, and E. Hanamura, Low Temp. Phys. **31**, 780 (2005).
[43] N. Kurti, *Selected Works of Louis Néel* (Taylor & Francis, New York, 1988).